Catalysis-Based Fluorometric Method for Trace Palladium Detection with Improved Convenience

Jessica M. Williams, Annelise K. Wanner, and Kazunori Koide*

Department of Chemistry, University of Pittsburgh

219 Parkman Avenue, Pittsburgh, Pennsylvania 15260, United States

koide@pitt.edu

Table of content figure

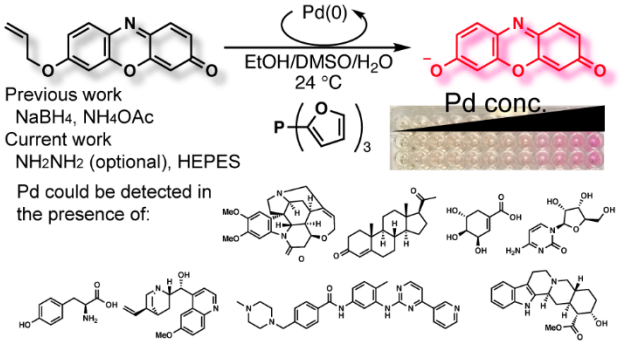

ABSTRACT: There is a need for rapidly estimating the quantities of trace palladium in synthetic samples. To address the need, we previously reported a rapid method based on the palladium-catalyzed conversion of nonfluorescent allyl resorufin ether to fluorescent resorufin in NH_4OAc buffer, which has been implemented in industry. The nuisance of the method is the need for $NaBH_4$ that cannot be stored in solution for more than half a day. Herein, we report the development of a $NaBH_4$-free method; the reaction is faster in HEPES buffer than in NH_4OAc buffer. The resulting colorimetric/fluorometric method enjoys high sensitivity and a greater degree of metal selectivity and is compatible with many drug-like molecules, except those containing sulfur. Unlike the previous method, all the assay solutions can be stored for weeks to months, potentially enabling more widespread use of the palladium detection method in the synthetic community.

KEYWORDS: allylic compound, palladium, high throughput, fluorescence

INTRODUCTION

Palladium is the most frequently used heavy metal in chemical synthesis, including pharmaceutical production.[1-6] To comply with governmental safety standards for the purity of active pharmaceutical ingredients (APIs), the palladium concentration in the solid state of APIs must be generally below 10 parts per million (ppm). Such requirement poses a challenge for process and analytical chemists, because the palladium content must be below 0.001% relative to the API by weight and yet must be quantified in the presence of the API in large excess (up to 10 000 fold). To overcome interference by the APIs and quantify trace metals, the choice of an analytical technique has been primarily limited to inductively coupled plasma mass spectrometry (ICP-MS). It should be noted that other technologies, such as neutron activation analysis,[7] are also used in some instances. As the synthetic community is shifting toward high throughput discoveries and chemical synthesis,[8-14] metal analysis must also be high throughput. However, currently used analytical methods are low throughput.

Fluorometric and colorimetric methods are amenable to high throughput analyses with the advent of multiplex plate readers. Currently, O-deallylation[15-36] and O-depropargylation[37-41] are the two widespread platforms to develop probes for palladium.[42-45] Despite over 100 publications on the development of palladium detection by fluorescence or color, the only technologies that are used in the pharmaceutical industry are the deallylation of either allyl Pittsburgh Green ether[24] or resorufin allyl ether (RAE) in the presence of tri(2-furyl)phosphine (TFP) and ammonium acetate (Figure 1a).[27,30] RAE may be more convenient than allyl Pittsburgh Green ether because the RAE method provides both colorimetric and fluorometric measurements and visualization. We previously published three variants with RAE,[27,31,35] and the first generation method has been routinely practiced at Merck Research Laboratories. These methods had shortcomings: first, sodium borohydride in aqueous sodium hydroxide (Figure 1b) is difficult to use.[27,30,35] More specifically, although a solution of sodium borohydride in 10 N sodium hydroxide is commercially available, we found it to be unreactive. This is because sodium borohydride in aqueous sodium hydroxide degrades in a few days.[46] Additionally, sodium hydroxide reacts with RAE if pH is not adjusted properly, generating false data.[35] Sodium hydroxide cannot be

omitted because sodium borohydride in non-basic water degrades within a few hours.[35] Therefore, a solution of sodium borohydride in aqueous sodium hydroxide must be prepared on the same day for reproducible results. Second, when we replaced sodium borohydride with hydrazine, the buffer salt was ammonium acetate (Figure 1c), but this buffer salt does not efficiently neutralize acids in API samples.[31] Third, replacing sodium borohydride with hydrazine substantially retarded the deallylation reaction, making the technique less sensitive. In the current manuscript, we describe the fourth-generation technology with RAE to quantify palladium, overcoming some of these disadvantages (Figure 1d). Although resorufin can be used for both colorimetry and fluorometry, we chose fluorescence as a readout because absorption is often inaccurate when trace insoluble materials are not removed from samples and because many APIs absorb light while few emit light.

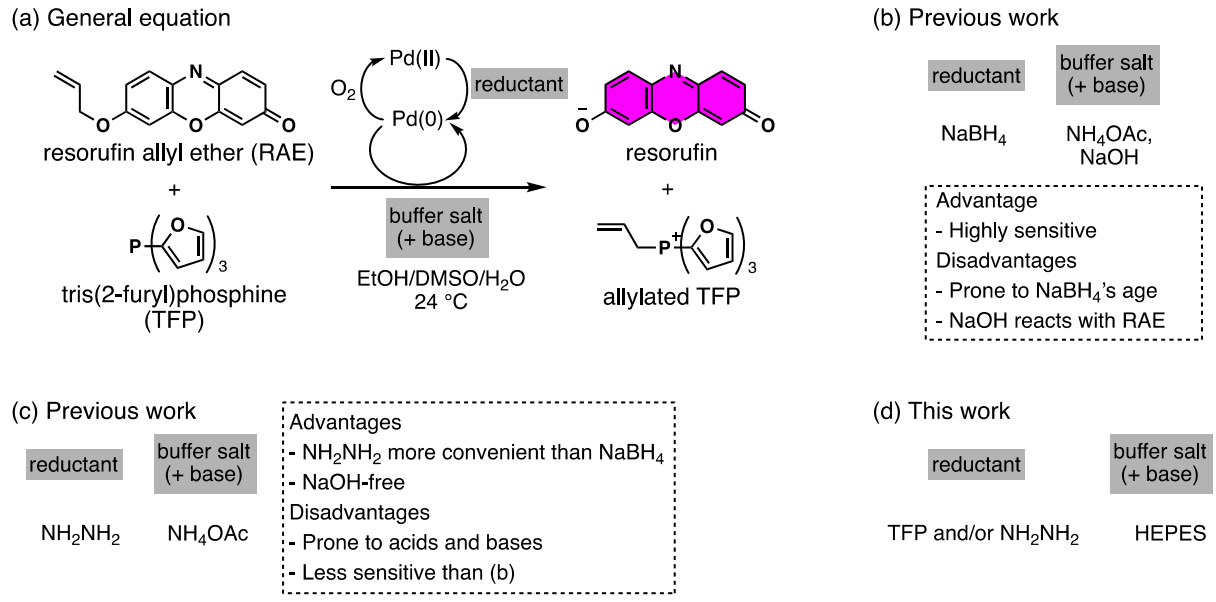

Figure 1. (a) General equation for the previous and current methods. (b) A previous method with $NaBH_4$, NaOH, and NH_4OAc. (c) A previous method with NH_2NH_2 and NH_4OAc. (d) This work with NH_2NH_2 and HEPES buffer.

RESULTS

Buffer Salts. In the quest for a more robust buffer with similar or better sensitivity for palladium, we performed the palladium-catalyzed deallylation of RAE in 200 mM 4-(2-hydroxyethyl)-1-piperazineethanesulfonic acid (HEPES), Tris, phosphate, and ammonium acetate (as a reference) buffers. A 1:12:12 v/v/v DMSO/water/ethanol solvent system was used to dissolve both organic and inorganic buffer salts. Figure 2a shows that the deallylation reaction was at least twice as fast in HEPES and phosphate buffers as in ammonium acetate buffer. Moreover, HEPES and phosphate buffers are more resistant than ammonium acetate buffer to the addition of acid or base. With high concentrations of phosphate ions in water-organic solvent mixtures, phase separation was frequently observed. Therefore, we chose HEPES as the new buffer system.

Reducing Agents. Next, we compared sodium borohydride and hydrazine to keep palladium in its reduced and catalytically active form, palladium(0), under air atmosphere during the assays. Hydrazine is preferred over sodium borohydride because it provides a non-effervescent protocol and its solution can be stored for months. Figure 2b shows a comparison between the previous method with sodium borohydride in the ammonium acetate buffer and the new method with hydrazine in HEPES buffer (the concentrations of hydrazine and HEPES were chosen after the following optimizations). The reaction rate was nearly negligible without reductants and was high with sodium borohydride in ammonium acetate buffer. We discovered that in HEPES buffer, an additional reductant was not critical, although hydrazine moderately accelerated the deallylation. Sodium borohydride was incompatible with HEPES buffer as manifested by rapid evolution of hydrogen gas. For a reason that is not yet clear, TFP appears to be an efficient reducing agent for palladium in HEPES buffer. From the result shown in Figure 2b, we decided to include hydrazine as a reductant in the assay solution. Switching from sodium borohydride to hydrazine is an improvement in convenience because hydrazine solutions can be stored for many months while sodium borohydride solutions must be prepared within 8 h prior to an assay due to their short shelf life.[46]

Concentrations of Components. Having established hydrazine, TFP, and HEPES as the ingredients, we opted to find the optimal concentrations for these components. We hypothesized that there might be an interplay between hydrazine and HEPES in the catalytic cycle (e.g., competitive or cooperative binding for palladium). Therefore, a combinatorial assay was conducted as shown in Figure 2c. The trend indeed showed mutual dependence; the worse performance (magenta-purple-blue) was observed diagonally in the heatmap. The higher HEPES concentrations were better; however, for users' convenience, we chose to limit the highest concentration to be 500 mM because the most concentrated pH 7 HEPES buffer solutions from commercial sources are 1 M. With HEPES at 500 mM, the hydrazine concentration was found to be optimal in the 53–79 mM range. Therefore, we chose to use 60 mM hydrazine in a 500 mM HEPES pH 7.0 buffer. Importantly, hydrazine at this concentration should not cause safety concerns according to the literature.[47]

In the next round of optimizations, we examined the deallylation efficiency as a factor of TFP concentration (Figure 2d). The reaction progression was nearly undetectable with 13 μM TFP. In our previous work, the reaction rate increased gradually as the TFP concentration increased.[31,48] The current method required far less TFP (20–44 μM). The downward trend above 44 μM is probably due to the formation of coordinatively saturated palladium species *in situ*.

As for the dependence on the RAE concentration, we previously observed Michaelis-Menten-type saturation kinetics.[35] The current method shows a substrate inhibition model (Figure 2e). Although the reaction rate was optimal when the RAE concentration was in the 11–25 μM range, we chose 50 μM RAE to avoid rapid regression of the reaction rate as the substrate is consumed during assay.

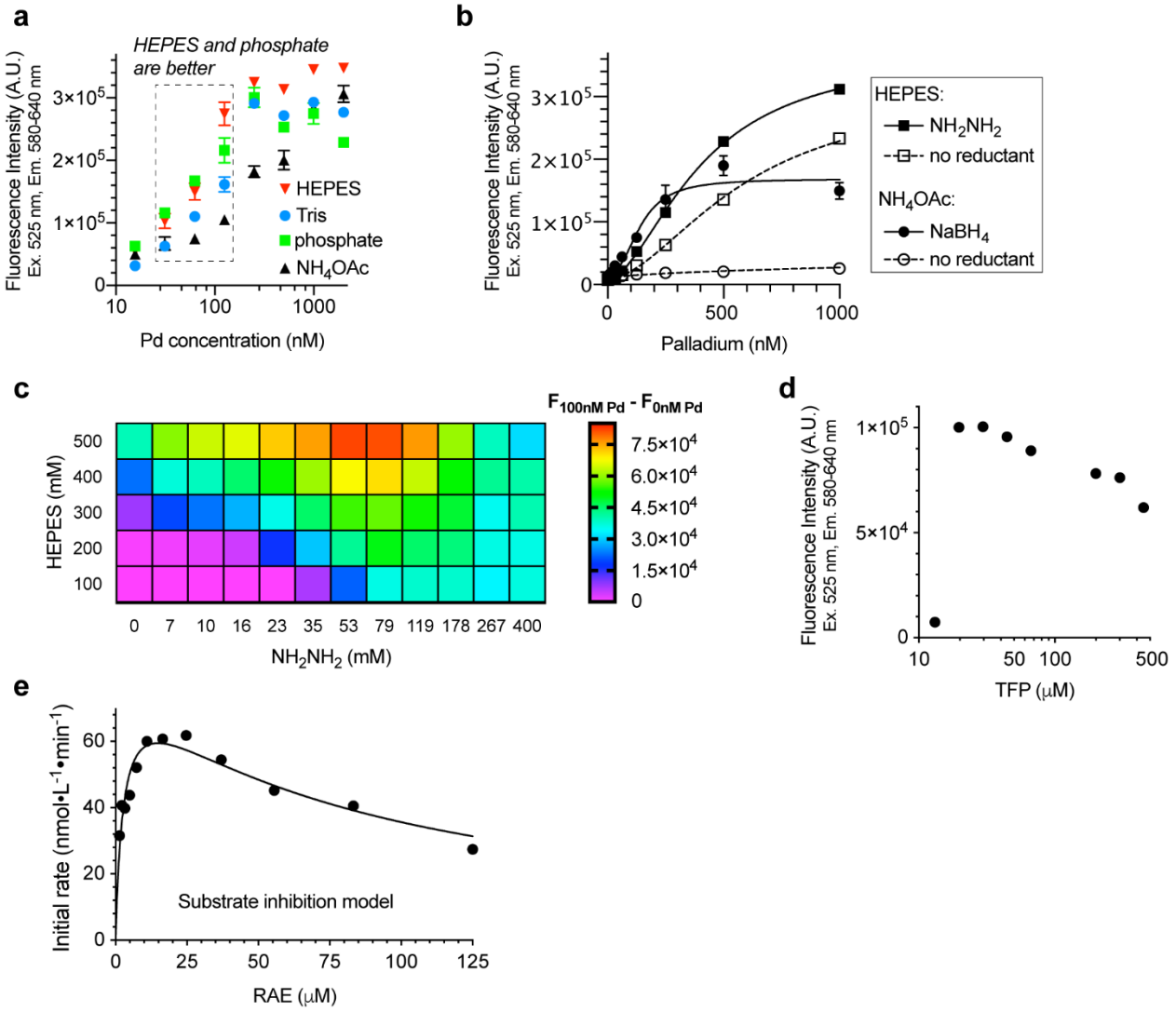

Figure 2. (a) Comparison of four pH 7 buffers. Conditions: 30 μM RAE, 180 μM TFP, 20 mM $NaBH_4$, 75 mM NaOH, 2.0, 3.9, 7.8, 16, 31, 63, 130, 250, 500, 1000, or 2000 nM Pd, 200 mM NH_4OAc, phosphate pH 7.0 buffer, HEPES pH 7.0 buffer, or Tris pH 7.0 buffer, 2:25:23 v/v/v DMSO/H_2O/EtOH, *n* = 3, 30 min, 24 °C. (b) Comparison of the NH_4OAc and $NaBH_4$ system of the 3rd generation colorimetric method with HEPES and NH_2NH_2 for reactivity. Conditions: 50 μM RAE, 40 or 180 μM TFP, 0 or 20 mM $NaBH_4$, 0 or 60 mM NH_2NH_2,80 mM NaOH, 0, 2.0, 3.9, 7.8, 16, 31, 63, 130, 250, 500, or 1000 nM Pd, 200 mM NH_4OAc or 500 mM HEPES pH 7.0 buffer, 1:6:3 or 1:5:4 v/v/v DMSO/H_2O/EtOH, *n* = 3, 12 min, 24 °C. (c) Combinatorial optimization of HEPES and NH_2NH_2 concentrations. Conditions: 30 μM RAE, 180 μM TFP, 400, 270, 180, 120, 80, 53, 35, 23, 16, 10, 6.9, or 0 mM NH_2NH_2, 0 or 100 nM Pd, 500, 400, 300, 200, 100 mM HEPES, 1:6:3 v/v/v DMSO/H_2O/EtOH; *n* = 1, 30 min, 24 °C. (d) Effect of TFP concentration. Conditions: 30 μM RAE, 13, 20, 30, 44, 67, 200, 300, or 450 μM TFP, 60 mM NH_2NH_2, 125 nM Pd, 500 mM HEPES, 1:6:3 v/v/v DMSO/H_2O/EtOH; *n* = 1, 30 min, 24 °C. (e) Relationship between **s**ubstrate concentration and reaction rate. Conditions: 1.4, 2.2, 3.3, 4.9, 7.3, 11, 16, 25, 37, 56, 83, or 125 μM RAE, 40 μM TFP, 60 mM NH_2NH_2, 500 mM HEPES pH 7.0 buffer, 1:6:3 v/v/v DMSO/H_2O/EtOH, *n* = 1, 15 min, 24 °C.

Metal Selectivity and Interference. With 50 μM RAE, 40 μM TFP, and 60 mM hydrazine in 500 mM HEPES in 1:6:3 v/v/v DMSO/water/ethanol, we evaluated metal selectivity (Figure 3a). Our previous method showed high metal selectivity, with platinum being the second most reactive metal. More quantitatively, the selectivity between palladium and platinum was 10:1.[35] The current method showed a higher selectivity between these two metals, 118:1 (= (112449-9932)/(10800-9932)). Next, metal interference was studied with 11.5

equivalents of other metals relative to palladium (Figure 3b). Mercury ions were found to have a negative effect on palladium quantification, possibly due to mercury-palladium amalgam formation. Gold and platinum showed 27–35% stronger signals. Therefore, when gold or platinum is expected to be in large excess compared to palladium, the interpretation of the data would require additional caution, and an independent analysis with ICP-MS is recommended.

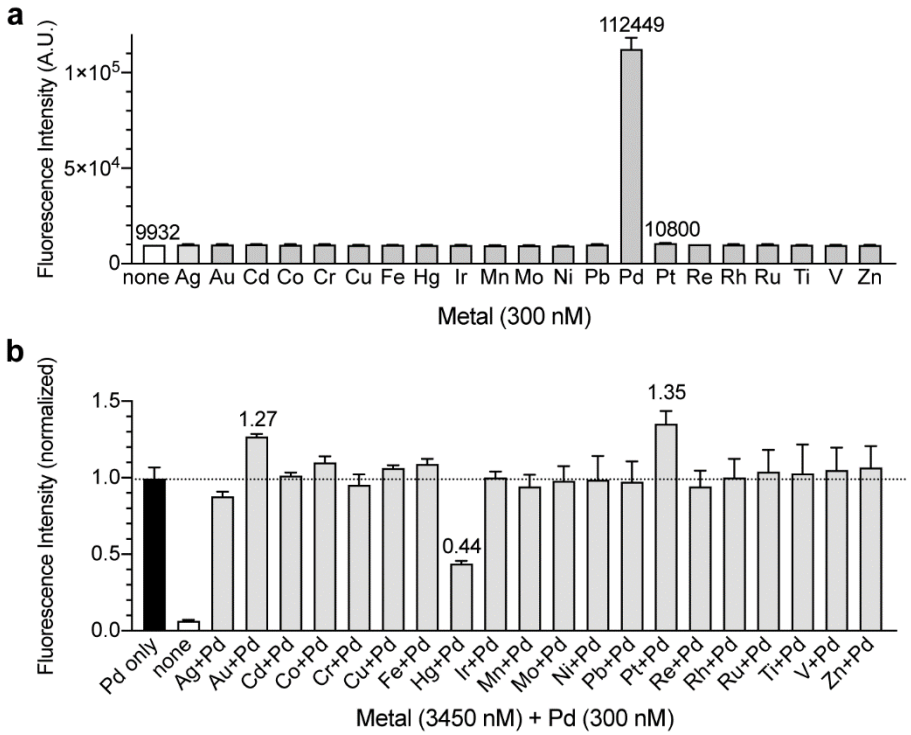

Figure 3. (a) Metal selectivity among period 4, 5, and 6 d-transition metals. Conditions: 50 μM RAE, 40 μM TFP, 60 mM NH_2NH_2, 300 nM metal or no metal, 500 mM HEPES pH 7.0 buffer, 1:6:3 v/v/v DMSO/H_2O/EtOH, *n* = 3, 30 min, 24 °C. (b) Metal Interference with period 4, 5, and 6 d-transition metals. Conditions: 50 μM RAE, 40 μM TFP, 60 mM NH_2NH_2, 3450 nM metal with 300 nM Pd, no metal, or 300 nM Pd with no other metal, 500 mM HEPES pH 7.0 buffer, 1:6:3 v/v/v DMSO/H_2O/EtOH, *n* = 3, 30 min, 24 °C.

Reaction Rates and Temperatures. Because the assay technology is catalysis-based, kinetic insights would help understand how perturbation of assay conditions might affect the assay outcome. In our previous study with allyl Pittsburgh Green ether, TFP, and sodium borohydride in a mixture of DMSO and pH 7 phosphate buffer, the kinetic profile consisted of three kinetic regimes.[48] Specifically, the activation energy of enthalpy was positive, near zero, and negative, in low, medium, and high temperature ranges, respectively.[48] The Eyring plot in Figure 4a indicates that the current method operates in the same set of three kinetic regimes. At ambient temperature, the reaction kinetics are under regime 1 (Figure 4b), meaning that the turnover-limiting step is presumably the oxidative addition of palladium to form π-allylpalladium intermediate. Although other regimes are not directly relevant to the present method, we attribute the turnover limiting steps of regimes 2 and 3 to be the nucleophilic attack of the π-allylpalladium intermediate and the association of a palladium catalyst to

the olefin, respectively.[48] A main point of these data is that assay solutions may be warmed up to 333K but above this temperature, the kinetic regime will change, and the quantification may require further calibration.

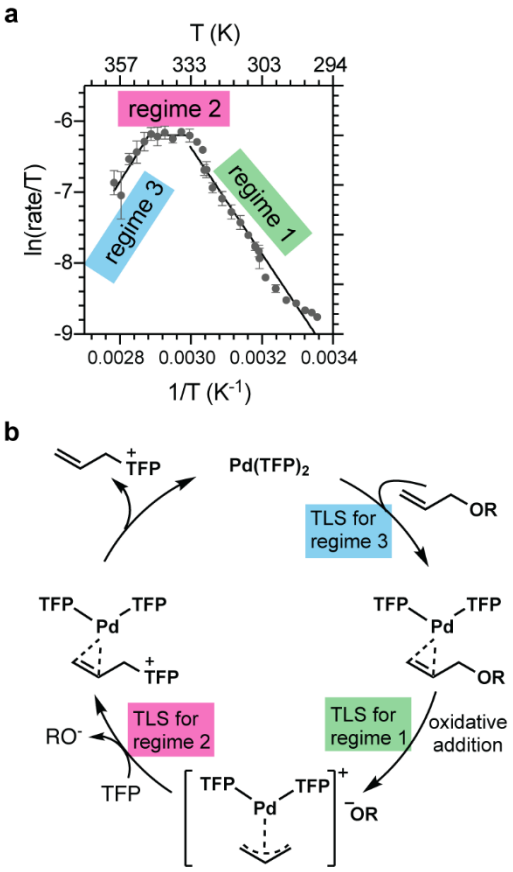

Figure 4. (a) Eyring-inspired plot; the maximum studied temperature was 86 °C as this is near the boiling point for a binary mixture of 2:3 EtOH/water.[49] Conditions: 50 μM RAE, 40 μM TFP, 60 mM NH_2NH_2, 50 nM or 0 nM Pd, 500 mM HEPES pH 7.0 buffer, 1:6:3 v/v/v DMSO/H_2O/EtOH, *n* = 5, 30 min, 25–86 °C. (b) Catalytic cycle of the palladium-catalyzed deallylation of RAE and turnover-limiting steps (TLSs).

Quantification of Palladium in API Matrix. For the assay to be useful during the process of metal scavenging, users wish to prioritize purification protocols with relative concentrations of palladium in various samples and not necessarily to find the absolute contents of palladium. Nonetheless, it is important to be aware of the dynamic range for the semi-quantification technology for palladium. The correlation between palladium concentrations and fluorescence intensities is shown in Figure 5 (in box). This graph shows that palladium quantification should be limited to the 0–500 nM range in the final assay solutions; if the final palladium concentrations exceed 500 nM, the original samples should be further diluted.

With this standard curve, we proceeded to evaluate the utility of the method in the presence of APIs and API-like compounds in large excess (800 – 10 000 fold). Known amounts of palladium were added to solutions of brucine, progesterone, shikimic acid, Imatinib™, cytidine, tyrosine, yohimbine, quinine, L-ascorbate, N-acetylcysteine, diphenylthiourea, and biotin. The resulting samples represent 0–1215 ppm palladium in the solid states of these mock APIs. Given the linear range of the semi-quantification technology, we chose to perform

assays with the concentration of APIs at either 0.1 or 0.01 mg/mL. For example, when the APIs are at the 0.1 mg/mL concentration, 0.44, 1.3, 4.0, 5.0, 12, 15, 45, 135, and 405 ppm palladium samples correspond to 0.4 0.42, 1.3, 3.8, 4.7, 11.3, 14.1, 42.3, 127, and 381 nM palladium concentrations in the assay solutions, respectively. The 1215 ppm palladium samples were used at the 0.01 mg/mL concentration in the assay, which is the equivalent of 114 nM palladium in solution.

Figure 5 shows that the fluorescence method was compatible with brucine, progesterone, shikimic acid, Imatinib™, cytidine, tyrosine, yohimbine, quinine, and L-ascorbate, while it was interfered by N-acetylcysteine, diphenylthiourea, and biotin. The interference is presumably because the sulfur atoms strongly coordinate palladium to suppress its catalytic activity. It should be noted that the third-generation method with sodium borohydride was effective with biotin (N-acetylcysteine and diphenylthiourea were not tested).[35] The robustness of the third-generation method may be attributed to palladium's stronger affinity for hydride than for sulfur. Nonetheless, if samples do not contain sulfides or thiourea (thiols are unlikely to be present in APIs), the fourth-generation method is expected to be useful for semi-quantifying palladium.

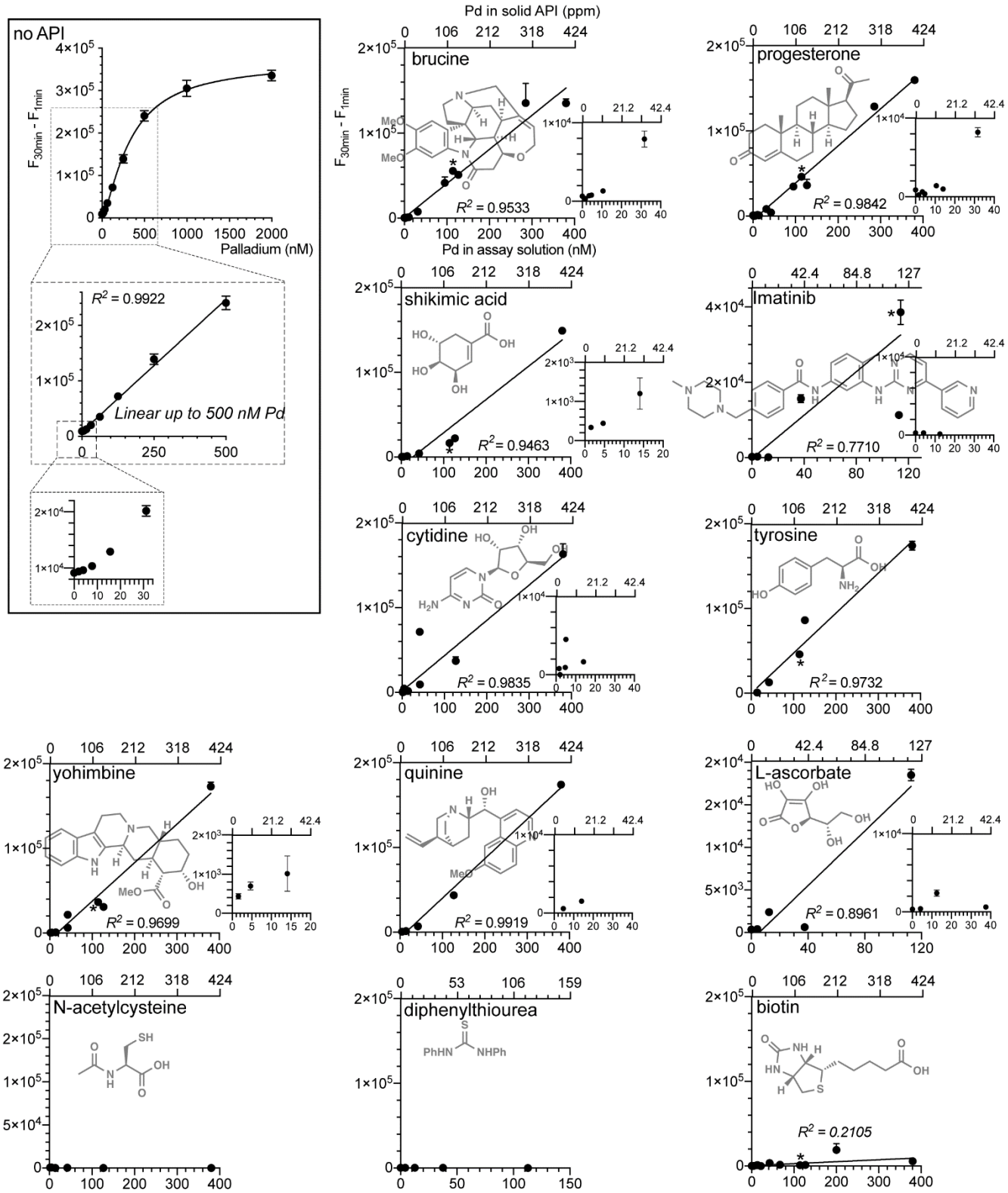

Figure 5. Conditions: 50 μM RAE, 40 μM TFP, 60 mM NH_2NH_2, 0, 2.0, 3.9, 7.8, 16, 31, 63, 130, 250, 500, 1000, or 2000 nM Pd, 500 mM HEPES pH 7.0 buffer, 1:6:3 v/v/v DMSO/H_2O/EtOH, *n* = 3, 30 min, 24 °C. Correlation graph. Mock APIs tested: brucine, progesterone, shikimic acid, Imatinib™, cytidine, tyrosine, yohimbine, quinine, L-ascorbate, N-acetylcysteine, diphenylthiourea, and biotin. Conditions: 50 μM RAE, 40 μM TFP, 60 mM NH_2NH_2, 0, 0.47, 1.4, 4.3, 4.7, 13, 14, 42, 114, 130, 380 nM Pd with 0.1 (without asterisks) or 0.01 (with asterisks) mg/mL API, 500 mM HEPES pH 7.0 buffer, 1:6:3 v/v/v DMSO/H_2O/EtOH (200 μL), *n* = 2-3, 30 min, 25 °C.

CONCLUSIONS

In conclusion, we have developed a fourth-generation optical method with RAE to estimate palladium concentrations in highly functionalized organic molecules at the 5–1215 ppm palladium levels. HEPES buffer proved to be more suitable than ammonium acetate buffer, and sodium borohydride could be replaced by hydrazine, or completely omitted, without loss of sensitivity. The Eyring plot study showed that the current protocol is in the regime 1 kinetic profile. As long as the technology is used with the upper limit of quantification in mind, relative fluorescence intensities can be used to prioritize metal-removing processes in a high throughput manner. To summarize the strengths and weaknesses of the third and fourth generation methods, the third generation is robust and benefits from the stop-and-go technology[27,35] and has already been implemented in flow chemistry,[30] but the preparation of sodium borohydride is a nuisance. The fourth generation enjoys continuous catalysis and long-term storage of stock solutions because it does not require sodium borohydride but is incompatible with APIs containing Lewis-basic sulfur.

EXPERIMENTAL SECTION

Materials and Methods. Water used in this study was purified by a Barnstead Nanopure Diamond Lab Water System. Reagent-grade DMSO was used without purification. Ethanol was USP-grade 200 proof. Trace-metal grade hydrochloric acid was purchased from Fisher. RAE was synthesized according to the published procedure[27] and stored at ambient temperature away from light. TFP was purchased from Fisher, and its solutions in DMSO were stabilized by hydroquinone and stored at ambient temperature in amber vials. Hydrazine hydrate (80%) was purchased from Fisher and stored at -20 °C. Sodium borohydride pellets (1.00 g per pellet) were purchased from Fisher. The 1.25 M phosphate pH 7.0 buffer, 1.0 M Tris pH 7.0 buffer, and the 1.0 M HEPES pH 7.0 buffer were purchased from Fisher and stored at 24 °C.

All metal standard solutions were Atomic Absorption Spectroscopy (AAS) grade unless specified otherwise. Molybdenum standard solution was purchased from Crescent, gold standard solution was purchased from Sigma-Aldrich, and the remaining metal standard solutions were purchased from Fisher. All the procedures for the preparation of stock solutions are described in the Supporting Information.

All the experiments were performed at ca. 24 °C unless stated otherwise. Fluorescence data were acquired using black round-bottomed 96-well plates and a Promega Biosystems Modulus II Microplate Reader (excitation 525 nm, emission 580–640 nm). GraphPad Prism 8.4.3 was used to generate graphs and perform statistical analyses.

Effects of Buffer Salts (Figure 2a). Solutions of 42.9 μM RAE and 286 mM NH_4OAc, phosphate, HEPES, or Tris buffer in 1:68:31 v/v/v DMSO/EtOH/water (140 μL per well) were transferred to a 96-well plate (Figure 6a). These wells were treated with a solution of either 0, 20, 39, 78, 160, 310, 630, 1300, 2500, 5000, 10 000, or 20 000 nM palladium in diluent **1** (1:4 v/v DMSO/water with 0.5 M HCl) (20 μL per well) followed by a

solution of 900 μM TFP, 100 mM $NaBH_4$, and 400 mM NaOH in 7:93 v/v DMSO/water (40 μL per well). Fluorescence data were acquired immediately after the additions and after 30 min.

Comparison between NH_2NH_2 in HEPES Buffer and $NaBH_4$ in NH_4OAc Buffer (Figure 2b). Solutions of 71.4 μM RAE and either 714 mM HEPES buffer in 9:20:71 v/v/v DMSO/EtOH/water or 71.4 μM RAE and 286 mM NH_4OAc 9:60:31 v/v/v DMSO/EtOH/water (140 μL per well) were transferred to a 96-well plate (Figure 6b). These wells were treated with a solution of either 0, 20, 39, 78, 160, 310, 630, 1300, 2500, 5000, 10 000, or 20 000 nM palladium in diluent **1** (20 μL per well). The wells containing 71.4 μM RAE and 714 mM HEPES buffer were treated with a solution of either 200 μM TFP and 300 mM NH_2NH_2 7:93 v/v DMSO/EtOH, or a solution of 200 μM TFP in 7:93 v/v DMSO/EtOH (40 μL per well). The wells containing 71.4 μM RAE and 286 mM NH_4OAc were treated with either a solution of 900 μM TFP, 100 mM $NaBH_4$ and 400 mM NaOH in 7:50:43 v/v/v DMSO/EtOH/water, or a solution of 900 μM TFP and 400 mM NaOH in 7:50:43 v/v/v DMSO/EtOH/water (40 μL per well). Fluorescence data were acquired immediately after the additions and after 12 min.

Effects of HEPES and NH_2NH_2 Concentrations (Figure 2c). Solutions of 42.9 μM RAE and either 714, 571, 429, 285, or 143 mM HEPES buffer in 9:20:71 v/v/v DMSO/EtOH/water (140 μL per well) were transferred to two 96 well-plates (Figure 6c). Both plates were then treated with 900 μM TFP and either 2000, 1333, 889, 593, 395, 263, 176, 117, 78, 52, 35, or 0 mM NH_2NH_2 in 7:93 v/v DMSO/EtOH (40 μL per well). One plate was then treated with diluent **1** (20 μL per well); the remaining plate was treated with 1000 nM Pd solution in diluent **1** (20 μL per well). The fluorescence data were acquired immediately after addition and after 30 min.

Effects of TFP Concentrations (Figure 2d). A solution of 42.9 μM RAE and 714 mM HEPES buffer in 9:20:71 v/v/v DMSO/EtOH/water (140 μL per well) was transferred to a 96 well-plate (Figure 6d). Solutions of either 0, 20, 39, 78, 160, 310, 630, 1300, 2500, 5000, 10 000, or 20 000 nM Pd in diluent **1** (20 μL per well) were added to the wells. The wells were then treated with a solution of 300 mM NH_2NH_2 and either 2250, 1500, 1000, 667, 444, 296, 198, or 0 μM TFP in 7:93 v/v DMSO/EtOH (40 μL per well). Fluorescence data were acquired immediately after the additions and after 30 min.

Effects of RAE Concentrations (Figure 2e). A solution of 139, 92.6, 61.7, 41.2, 27.4, 18.3, 12.2, 8.13, 5.42, 3.62, or 2.41 μM RAE, 40 μM TFP, 60 mM NH_2NH_2, and 500 mM HEPES pH 7.0 buffer in 9:35:56 v/v/v DMSO/EtOH/water (180 μL per well) was added to a 96-well plate (Figure 6e). The wells were then treated with either 0 or 1000 nM Pd in diluent **1** (20 μL per well). Fluorescence data were acquired immediately after addition and after 15.5 min.

Metal Selectivity (Figure 3a). A solution of 71.4 μM RAE and 714 mM HEPES buffer in 9:19:72 v/v/v DMSO/EtOH/water (140 μL per well) was transferred to a 96-well plate (Figure 6f). Then 3000 nM solutions of either Ag, Au, Cd, Co, Cr, Cu, Fe, Hg, Ir, Mn Mo, Ni, Pb, Pt, Re, Rh, Ti, V, Zn, or Pd in diluent **1** (20 μL per

well) were added to the plate. The wells were then treated with a solution of 200 µM TFP and 300 mM NH_2NH_2 in 7:93 v/v DMSO/EtOH (40 µL per well) Fluorescence data were acquired immediately after addition and after 30 min.

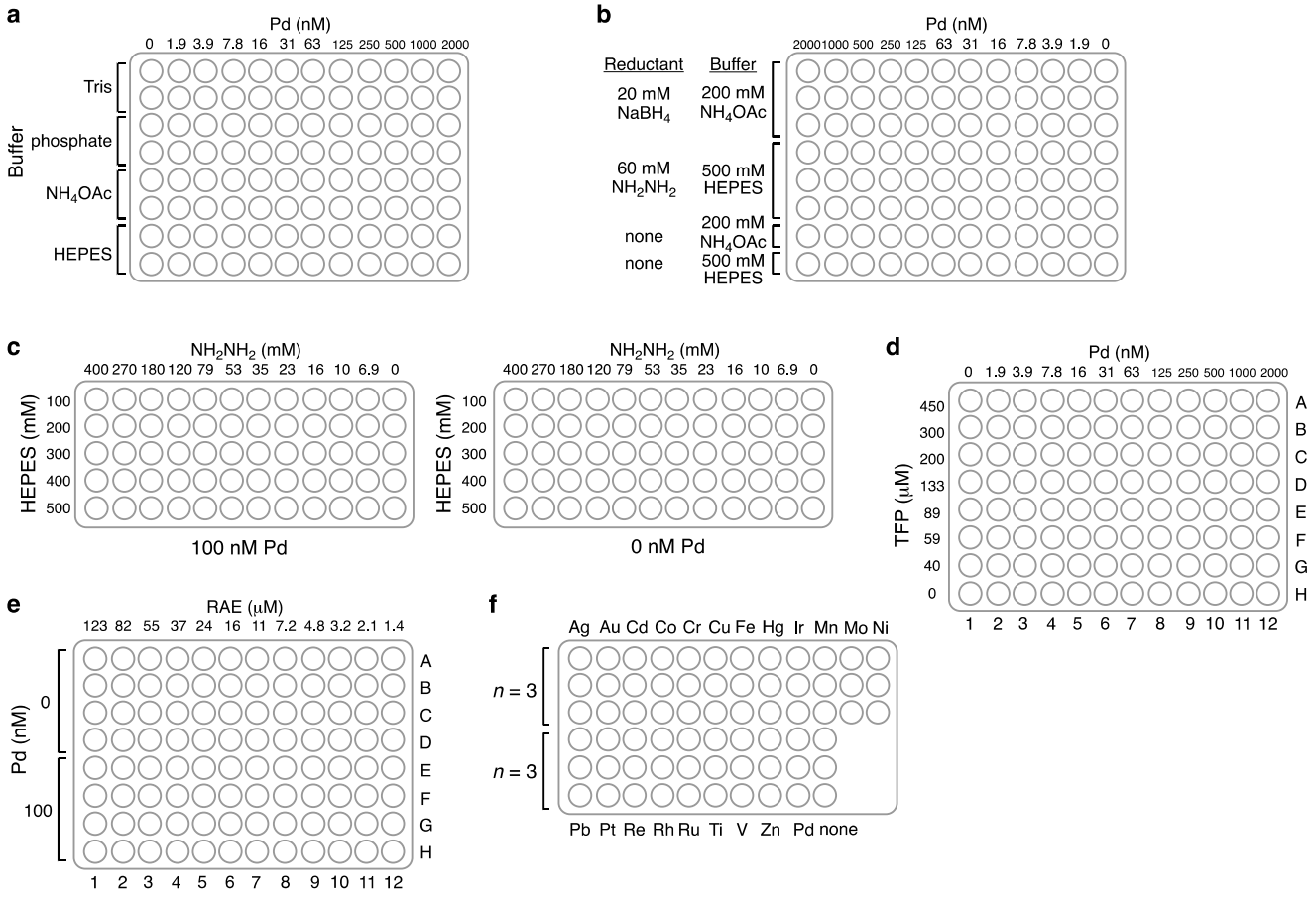

Figure 6. Plate maps.

Metal Interference (Figure 3b). A solution of 71.4 µM RAE and 714 mM HEPES buffer in 9:19:72 v/v/v DMSO/EtOH/water (140 µL per well) was transferred to a 96-well plate. A solution of either diluent **1**, 3000 nM Pd, or 3000 nM Pd and 34 500 nM Ag, Au, Cd, Co, Cr, Cu, Fe, Hg, Ir, Mn Mo, Ni, Pb, Pt, Re, Rh, Ti, V, or Zn (20 µL per well) was added to the wells. Subsequently, the wells were treated with a solution of 200 µM TFP and 300 mM NH_2NH_2 in 7:93 v/v DMSO/EtOH (40 µL per well). Fluorescence data were acquired immediately after addition and after 30 min.

Eyring Plot (Figure 4a). The reaction solution on ice (200 µL per tube) was transferred to 200-µL thin-walled PCR tubes, capped, and placed in the thermal cycler with 4 replicates per temperature. A 3-degree temperature increment was applied, with median temperature as indicated, spanning a 20-degree range. For example, for the data shown in Figure 4a, four reactions were set at 295.6, 299.0, 302.3, 305.7, 310.6, 314.0, 317.3, 320.7, 325.6, 329.0, 332.3, or 335.6 K, and the average and standard deviation were shown for each specific temperature. In the next experiment, the reactions were performed at 325.6, 329.0, 332.3, 335.6 340.7,

342.3, 344.0, 345.6, 347.3, 349.0, 350.6, and 352.3 K so that there is an overlap at 325.6, 329.0, 332.3, 335.6 K. If the overlapped range showed discrepancy, we repeated the experiment until the overlap was acceptable for normalization. After the indicated time for each experiment, the PCR tubes were removed from the thermal cycler, cooled to 0 °C on ice, and each solution (180 μL) was transferred to a 96-well plate to measure fluorescence. Moles of resorufin were calculated using the standard curve for resorufin. The natural log of the rate against the inverse of the temperature was plotted to afford an Eyring plot.

Correlation between Palladium Concentrations and Fluorescence Intensities without API (Figure 5). A solution of 71.4 μM RAE and 714 mM HEPES buffer in 11:15:74 v/v/v DMSO/EtOH/water (140 μL per well) was added to a 96-well plate. A solution of either 0, 19.6, 39.1, 78.1, 156, 313, 625, 1250, 2500, 5000, 10 000, or 20 000 nM Pd in diluent **1** (20 μL per well) was transferred to the 96-well plate. The wells were then treated with a solution of 200 μM TFP and 300 mM NH_2NH_2 in 1:96:3 v/v/v DMSO/EtOH/water (40 μL per well). Fluorescence data were acquired immediately after addition and after 30 min.

Correlation between Palladium Concentrations and Fluorescence Intensities in the Presence of APIs (Figure 5). A solution of 71.4 μM RAE and 714 mM HEPES buffer in 11:15:74 v/v/v DMSO/EtOH/water (140 μL per well) was added to a 96-well plate. The wells were treated with a solution of 1.0 mg/mL brucine, progesterone, shikimic acid, Imatinib™, cytidine, tyrosine, yohimbine, quinine, L-ascorbate, *N*-acetylcysteine, diphenylthiourea, or biotin with 0, 0.44, 1.3, 4, 5, 12, 15, 45, 135, or 405 ppm Pd in the solid API in diluent **1** (20 μL per well). For the API samples with 1215 ppm Pd in the solid state, 0.1 mg/mL API solutions were used instead to keep the fluorescence intensities within the linear range. The wells were then treated with a solution of 200 μM TFP and 300 mM NH_2NH_2 in 1:3:96 v/v/v DMSO/water/EtOH (40 μL per well). Fluorescence data were acquired immediately after addition and after 30 min.

ASSOCIATED CONTENT

The Supporting Information is available free of charge at http://pubs.acs.org/doi

Experimental procedures for the preparation of stock solutions, raw fluorescence data

AUTHOR INFORMATION

Corresponding Author

Kazunori Koide – Department of Chemistry, University of Pittsburgh, 219 Parkman Avenue, Pittsburgh, Pennsylvania 15260, United States; orcid.org/0000-0001-8894-8485

Email: koide@pitt.edu

Authors

Jessica M. Williams – Department of Chemistry, University of Pittsburgh, 219 Parkman Avenue, Pittsburgh, Pennsylvania 15260, United States; orcid.org/0000-0003-2266-322X

Annelise K. Wanner – Department of Chemistry, University of Pittsburgh, 219 Parkman Avenue, Pittsburgh, Pennsylvania 15260, United States; orcid.org/0000-0001-9791-5239

Author Contributions

J.M.W. and K.K. designed experiments. J.M.W. and A.K.W. performed experiments. All authors analyzed data. J.M.W. and K.K. wrote the manuscript.

ACKNOWLEDGMENTS

This work was supported by the US National Science Foundation (CHE-1506942 and CHE-1955758).

ABBREVIATIONS

Ac, acetyl; API, active pharmaceutical ingredient; DMSO, dimethyl sulfoxide; Et, ethyl; h, hour; HEPES, 4-(2-hydroxyethyl)-1-piperazineethanesulfonic acid; ICP-MS, inductively coupled plasma mass spectrometry; M, molar; min, minutes; ppm, parts per million; RAE, resorufin allyl ether; TFP, tri(2-furyl)phosphine

REFERENCES

(1) Nicolaou, K. C.; Bulger, P. G.; Sarlah, D. Palladium-catalyzed cross-coupling reactions in total synthesis. *Angew. Chem., Int. Ed.* **2005,** *44*, 4442–4489.
(2) Magano, J.; Dunetz, J. R. Large-scale applications of transition metal-catalyzed couplings for the synthesis of pharmaceuticals. *Chem. Rev.* **2011,** *111*, 2177–2250.
(3) Seechurn, C. C. C. J.; Kitching, M. O.; Colacot, T. J.; Snieckus, V. Palladium-catalyzed cross-coupling: A historical contextual perspective to the 2010 Nobel Prize. *Angew. Chem., Int. Ed.* **2012,** *51*, 5062–5085.
(4) *New trends in cross-coupling: Theory and applications*; Royal Society of Chemistry, 2015.
(5) Brow, D. G.; Boström, J. Analysis of past and present synthetic methodologies on medicinal chemistry: Where have all the new reactions gone? *J. Med. Chem.* **2016,** *59*, 4443–4458.
(6) Boström, J.; Brown, D. G.; Young, R. J.; Keserü, G. M. Expanding the medicinal chemistry synthetic toolbox. *Nat. Rev. Drug Disc.* **2018,** *17*, 709–727.
(7) Tu, S.; Yusuf, S.; Muehlfeld, M.; Bauman, R.; Vanchura, B. The destiny of palladium: Development of efficient palladium analysis techniques in enhancing palladium recovery. *Org. Process Res. Dev.* **2019,** *23*, 2175–2180.
(8) Lin, S. S.; Dikler, S.; Blincoe, W. D.; Ferguson, R. D.; Sheridan, R. P.; Peng, Z. W.; Conway, D. V.; Zawatzky, K.; Wang, H.; Cernak, T.et al. Mapping the dark space of chemical reactions with extended nanomole synthesis and MALDI-TOF MS. *Science* **2018,** *361*, 569.
(9) Perera, D.; Tucker, J. W.; Brahmbhatt, S.; Helal, C. J.; Chong, A.; Farrell, W.; Richardson, P.; Sach, N. W. A platform for automated nanomole-scale reaction screening and micromole-scale synthesis in flow. *Science* **2018,** *359*, 429–434.
(10) Renom-Carrasco, M.; Lefort, L. Ligand libraries for high throughput screening of homogeneous catalysts. *Chem. Soc. Rev.* **2018,** *47*, 5038–5060.
(11) Isbrandt, E. S.; Sullivan, R. J.; Newman, S. G. High throughput strategies for the discovery and optimization of catalytic reactions. *Angew. Chem., Int. Ed.* **2019,** *58*, 7180–7191.
(12) Kim, H.; Gerosa, G.; Aronow, J.; Kasaplar, P.; Ouyang, J.; Lingnau, J. B.; Guerry, P.; Farès, C.; List, B. A multi-substrate screening approach for the identification of a broadly applicable Diels–Alder catalyst. *Nat. Commun.* **2019,** *10*, 770.
(13) Welch, C. J. High throughput analysis enables high throughput experimentation in pharmaceutical process research. *React. Chem. Eng.* **2019,** *4*, 1895-1911.
(14) Bayly, A. A.; McDonald, B. R.; Mrksich, M.; Scheidt, K. A. High-throughput photocapture approach for reaction discovery. *Proc. Natl. Acad. Sci. U.S.A.* **2020,** *117*, 13261–13266.
(15) Song, F. L.; Garner, A. L.; Koide, K. A highly sensitive fluorescent sensor for palladium based on the allylic oxidative insertion mechanism. *J. Am. Chem. Soc.* **2007,** *129*, 12354–12355.
(16) Garner, A. L.; Koide, K. Oxidation state-specific fluorescent method for palladium(II) and platinum(IV) based on the catalyzed aromatic Claisen rearrangement. *J. Am. Chem. Soc.* **2008,** *130*, 16472–16473.
(17) Garner, A. L.; Koide, K. Studies of a fluorogenic probe for palladium and platinum leading to a palladium-specific detection method. *Chem. Commun.* **2009**, DOI:10.1039/B814197e 10.1039/B814197e, 86–88.

(18) Garner, A. L.; Song, F. L.; Koide, K. Enhancement of a catalysis-based fluorometric detection method for palladium through rational fine-tuning of the palladium species. *J. Am. Chem. Soc.* **2009,** *131*, 5163–5171.
(19) Song, F. L.; Carder, E. J.; Kohler, C. C.; Koide, K. Studies toward an ideal fluorescence method to measure palladium in functionalized organic molecules: effects of sodium borohydride, temperature, phosphine ligand, and phosphate ions on kinetics. *Chem.-Eur. J.* **2010,** *16*, 13500–13508.
(20) Baker, M. S.; Phillips, S. T. A two-component small molecule system for activity-based detection and signal amplification: Application to the visual detection of threshold levels of Pd(II). *J. Am. Chem. Soc.* **2011,** *133*, 5170–5173.
(21) Jiang, J.; Jiang, H. E.; Liu, W.; Tang, X. L.; Zhou, X.; Liu, R. T.; Liu, W. S. A colorimetric and ratiometric fluorescent probe for palladium. *Org. Lett.* **2011,** *13*, 4922–4925.
(22) Inamoto, K.; Campbell, L. D.; Doi, T.; Koide, K. A highly sensitive fluorescence method reveals the presence of palladium in a cross-coupling reaction mixture not treated with transition metals. *Tetrahedron Lett.* **2012,** *53*, 3147–3148.
(23) Li, D.; Campbell, L. D.; Austin, B. A.; Koide, K. Detection of trace palladium in flasks and metal reagents using a fluorogenic Tsuji-Trost reaction. *ChemPlusChem* **2012,** *77*, 281–283.
(24) Bu, X. D.; Koide, K.; Carder, E. J.; Welch, C. J. Rapid analysis of residual palladium in pharmaceutical development using a catalysis-based fluorometric method. *Org. Process Res. Dev.* **2013,** *17*, 108–113.
(25) Williams, J. M.; Koide, K. A high-throughput method to detect palladium in ores. *Ind. Eng. Chem. Res.* **2013,** *52*, 8612–8615.
(26) Kitley, W. R.; Maria, P. J. S.; Cloyd, R. A.; Wysocki, L. M. Synthesis of high contrast fluorescein-diethers for rapid bench-top sensing of palladium. *Chem. Commun.* **2015,** *51*, 8520–8523.
(27) Koide, K.; Tracey, M. P.; Bu, X.; Jo, J.; Williams, M. J.; Welch, C. J. A competitive and reversible deactivation approach to catalysis-based quantitative assays. *Nat. Commun.* **2016,** *7*, 10691.
(28) Liu, Y. C.; Xiang, K. Q.; Guo, M.; Tian, B. Z.; Zhang, J. L. A coumarin-based fluorescent probe for the fast detection of Pd^0 with low detection limit. *Tetrahedron Lett.* **2016,** *57*, 1451–1455.
(29) Bhanja, A. K.; Mishra, S.; Das Saha, K.; Sinha, C. A fluorescence 'turn-on' chemodosimeter for the specific detection of Pd^{2+} by a rhodamine appended Schiff base and its application in live cell imaging. *Dalton Trans.* **2017,** *46*, 9245–9252.
(30) Bu, X.; Williams, M.; Jo, J.; Koide, K.; Welch, C. J. Online sensing of palladium in flowing streams. *Chem. Commun.* **2017,** *53*, 720–723.
(31) Nieberding, M.; Tracey, M. P.; Koide, K. Noneffervescent method for catalysis-based palladium detection with color or fluorescence. *ACS Sens.* **2017,** *2*, 1737–1743.
(32) Xia, Q. F.; Feng, S. M.; Liu, D. D.; Feng, G. Q. A highly selective and sensitive colorimetric and near-infrared fluorescent turn-on probe for rapid detection of palladium in drugs and living cells. *Sens. Actuators, B* **2018,** *258*, 98–104.
(33) Zhang, Y.; Li, Y. X.; Yang, X. F.; Ding, Y. M.; Zhao, Z. S.; Liu, X. L.; Yang, Z.; Cui, Y. A single-state fluorescent with bright white-light emission in the solid station and aggregation-induced emission enhancement compound for Pd^0 detection. *Talanta* **2018,** *179*, 177–185.
(34) Jin, M.; Wei, L.; Yang, Y.; Run, M.; Yin, C. A new turn-on fluorescent probe for the detection of palladium(0) and its application in living cells and zebrafish. *New J. Chem.* **2019,** *43*, 548–551.
(35) Lukomski, L.; Pohorilets, I.; Koide, K. Third-generation method for high-throughput quantification of trace palladium by color or fluorescence. *Org. Process Res. Dev.* **2020,** *24*, 85–95.
(36) Sóvári, D.; Keserű, G. M.; Ábrányi-Balogh, P. Application of boroisoquinoline fluorophores as chemodosimeters for fluoride ion and Pd (0). *Materials* **2020,** *13*, ARTN 199.
(37) Santra, M.; Ko, S. K.; Shin, I.; Ahn, K. H. Fluorescent detection of palladium species with an *O*-propargylated fluorescein. *Chem. Commun.* **2010,** *46*, 3964–3966.
(38) Chen, Y.; Chen, B.; Luo, D. J.; Cai, Y. Y.; Wei, Y. N.; Han, Y. F. A facile naphthalene-based fluorescent 'turn-on' chemodosimeter for palladium ions in aqueous solution. *Tetrahedron Lett.* **2016,** *57*, 1192–1195.
(39) Chen, Y.; Zhang, M. M.; Han, Y. F.; Wei, J. A depropargylation-triggered spontaneous cyclization based fluorescent "turn-on" chemodosimeter for the detection of palladium ions and its application in live-cell imaging. *RSC Adv.* **2016,** *6*, 8380–8383.
(40) Huo, F. J.; Zhang, Y. Q.; Kang, J.; Chao, J. B.; Zhang, Y. B.; Yin, C. X. A novel alkyne compound as a Pd(II) fluorescent probe in aqueous medium and its bioimaging. *Sens. Actuators, B* **2017,** *243*, 429–434.
(41) Zhang, X. P.; Yuan, Q.; Qi, Y. L.; Zheng, D. J.; Liu, Q. X.; Wang, B. Z.; Yang, Y. S.; Zhu, H. L. An umbelliferone-derivated fluorescent sensor for selective detection of palladium(II) from palladium(0) in living cells. *Spectrochim Acta A* **2019,** *220*, 117134.
(42) Li, H. L.; Fan, J. L.; Peng, X. J. Colourimetric and fluorescent probes for the optical detection of palladium ions. *Chem. Soc. Rev.* **2013,** *42*, 7943–7962.

(43) Koide, K. In *New trends in cross-coupling: Theory and applications*; Colacot, T. J., Ed.; Royal Society of Chemistry, 2015.
(44) Tracey, M. P.; Pham, D.; Koide, K. Fluorometric imaging methods for palladium and platinum and the use of palladium for imaging biomolecules. *Chem. Soc. Rev.* **2015,** *44*, 4769–4791.
(45) Balamurugan, R.; Liu, J. H.; Liu, B. T. A review of recent developments in fluorescent sensors for the selective detection of palladium ions. *Coord. Chem. Rev.* **2018,** *376*, 196–224.
(46) Lyttle, D. A.; Jensen, E. H.; Struck, W. A. A simple volumetric assay for sodium borohydride. *Anal. Chem.* **1952,** *24*, 1843–1844.
(47) Niemeier, J. K.; Kjell, D. P. Hydrazine and aqueous hydrazine solutions: Evaluating safety in chemical processes. *Org. Process Res. Dev.* **2013,** *17*, 1580–1590.
(48) Pohorilets, I.; Tracey, M. P.; LeClaire, M. J.; Moore, E. M.; Lu, G.; Liu, P.; Koide, K. Kinetics and inverse temperature dependence of a Tsuji–Trost reaction in aqueous buffer. *ACS Catal.* **2019,** *9*, 11720–11733.
(49) Aldrich, E. W.; Querfeld, D. W. Freezing and boiling points of the ternary system ethanol-methanol-water. *Ind. Eng. Chem.* **1931,** *23*, 708–711.